

OW-VISCap: Open-World Video Instance Segmentation and Captioning

Anwesa Choudhuri, Girish Chowdhary, and Alexander G. Schwing

University of Illinois at Urbana-Champaign
{anwesac2,girishc,aschwing}@illinois.edu

<https://anwesachoudhuri.github.io/OpenWorldVISCap/>

Abstract. Open-world video instance segmentation is an important video understanding task. Yet most methods either operate in a closed-world setting, require an additional user-input, or use classic region-based proposals to identify never before seen objects. Further, these methods only assign a one-word label to detected objects, and don't generate rich object-centric descriptions. They also often suffer from highly overlapping predictions. To address these issues, we propose Open-World Video Instance Segmentation and Captioning (OW-VISCap), an approach to jointly segment, track, and caption previously seen or unseen objects in a video. For this, we introduce open-world object queries to discover never before seen objects without additional user-input. We generate rich and descriptive object-centric captions for each detected object via a masked attention augmented LLM input. We introduce an inter-query contrastive loss to ensure that the object queries differ from one another. Our generalized approach matches or surpasses state-of-the-art on three tasks: open-world video instance segmentation on the BURST dataset, dense video object captioning on the VidSTG dataset, and closed-world video instance segmentation on the OVIS dataset.

1 Introduction

Open-world video instance segmentation (OW-VIS) involves detecting, segmenting and tracking previously seen or unseen objects in a video. This task is challenging because the objects are often never seen during training, are occasionally partly or entirely occluded, the appearance and position of these objects changes over time, and because the objects may leave the scene only to re-appear at a later time. Addressing these challenges to obtain an accurate method for OW-VIS that works online is crucial in fields like autonomous systems, and augmented as well as virtual reality, among others.

Some recent methods based on abstract object queries perform remarkably well for closed-world video instance segmentation [7, 13, 18, 50]. These works assume a fixed set of object categories during training and evaluation. However, it is unrealistic to assume that all object categories are seen during training. For example, in Fig. 1, the trailer truck (top row) highlighted in yellow, and the lawn mower (bottom row) highlighted in green, are never seen before during training.



Fig. 1: OW-VISCap is able to simultaneously detect, track and caption objects in the given video frames. The first example (top row) shows a road scene with a previously unseen trailer truck and cars which are seen during training. The second example (bottom row) shows a person on a lawn mower, and a dog on the grass. The lawn mower isn’t part of the training set. We generate meaningful object-centric captions even for objects never seen during training. The captions for unseen objects are underlined.

For this reason, open-world video instance segmentation (OW-VIS) has been proposed [2,10,27,28,39,44]. Current works on OW-VIS suffer from the following three main issues. Firstly, they often require a prompt, *i.e.*, additional input from the user, ground-truth or another network. The prompts can be in the form of points, bounding boxes or text. These methods only work when the additional inputs are available, making them less practical in the real-world. Prompt-less OW-VIS methods [2,10,27,28,39,44] sometimes rely on classic region-based object proposals [2,27,28,44], or only operate on one kind of object query for both the open- and the closed-world [10,39], which may result in sub-optimal results (shown later in Tab. 4). Secondly, all methods on video instance segmentation, closed- or open-world, assign a one-word label to the detected objects. However, a one word label is often not sufficient to describe an object. The ability to generate rich object-centric descriptions is important, especially in the open-world setting. DVOC-DS [58] jointly addresses the task of closed-world object detection and object-centric captioning in videos. However, it is not clear how DVOC-DS [58] can be extended to an open-world setting. Besides, the features from only the individual object trajectories are used for object-centric captioning in DVOC-DS [58], so the overall context from the entire video frames may be lost in this method. DVOC-DS [58] also struggles with very long videos, and cannot caption multiple action segments within a single object trajectory because the method produces a single caption for the entire object trajectory. Thirdly, some of the aforementioned works [7,8,13,18] suffer from multiple similar object queries resulting in repetitive predictions. Non-maximum suppression, or other post-processing techniques may be necessary to suppress the repetitions and highly overlapping false positives.

We address the three aforementioned issues through our Open-World Video Instance Segmentation and Captioning (OW-VISCap) approach: it simultaneously detects, segments and generates object-centric captions for objects in a video. Fig. 1 shows two examples in which our method successfully detects, segments and captions both closed- and open-world objects.

To address the first issue, our OW-VISCap combines the advantages of both prompt-based and prompt-less methods. We introduce open-world object queries, in addition to closed-world object queries used in prior work [8]. This encourages discovery of never before seen open-world objects without compromising the closed-world performance much. Notably, we do not require additional prompts from the ground truth or separate networks. Instead, we use equally spaced points distributed across the video frames as prompts and encode them to form open-world object queries, which enables discovery of new objects. The equally spaced points incorporate information from different spatial regions of the given video-frames. We also introduce a specifically tailored open-world loss to train the open-world object queries to discover new objects.

To address the second issue, OW-VISCap includes a captioning head to produce an object-centric caption for each object query, both open- and closed-world. We use masked cross attention in an object-to-text transformer in the captioning head to generate object-centric text queries, that are then used by a frozen large language model (LLM) to produce an object-centric caption. Note, masked attention has been used for closed-world object segmentation [7,8]. However, to our best knowledge it has not been used for object captioning before. The masked cross attention helps focus on the local object features, whereas the self attention in the object-to-text transformer incorporates overall context by looking at the video-frame features. Moreover, unlike DVOC-DS [58], we are able to handle long videos and multiple action segments within a single object trajectory because we process short video clips sequentially and combine the clips using CAROQ [13].

To address the third issue, we introduce an inter-query contrastive loss for both open- and closed-world object queries. It encourages the object queries to differ from one another. This prevents repetitive predictions and encourages novel object discovery in the open-world. Note that this contrastive loss also helps in closed-world video instance segmentation by automatically encouraging non-maximum suppression, and by removing highly overlapping false positive predictions.

To demonstrate the efficacy of our OW-VISCap on open-world video instance segmentation and captioning, we evaluate this approach on three diverse and challenging tasks: open-world video instance segmentation (OW-VIS), dense video object captioning (Dense VOC), and closed-world video instance segmentation (VIS). We achieve a performance improvement of $\sim 6\%$ on the previously unseen (uncommon) categories in the BURST [2] dataset for OW-VIS, and a $\sim 7\%$ improvement on the captioning accuracy for detected objects on the VidSTG [57] dataset for the Dense VOC task, while performing similar to the state-

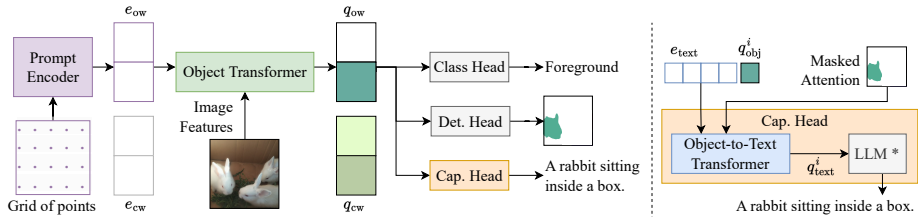


Fig. 2: The left figure shows an overview of our OW-VISCap (Sec. 3.1). We introduce open-world object queries q_{ow} (Sec. 3.2) and a captioning head (Sec. 3.3). The open-world object queries are generated by encoding a grid of points along the image-feature dimensions via a prompt encoder (shown in purple). The right figure details the captioning head (Sec. 3.3) for object-centric captioning. We use masked attention in the object-to-text transformer of the captioning head.

of-the-art on the closed-world VIS task on the OVIS data (our AP score is 25.4 as compared to a score of 25.8 for a recent VIS SOTA, CAROQ [13]).

2 Related Work

2.1 Open-world Video Instance Segmentation

Prompt-less methods. Several works have explored the open-world video instance segmentation problem without requiring initial prompts [2, 10, 28, 39, 44]. New objects are discovered based on an objectness score. Some works [2, 28] rely on classic region-based object proposals. However, recent query-based methods [10, 39] have shown to outperform those methods for object detection and segmentation. OW-VISFormer [39] proposes a feature enrichment mechanism and a spatio-temporal objectness module to distinguish the foreground objects from the background. Different from our work, they operate on one type of object query. Also orthogonal to our work is DEVA [10], which develops a class-agnostic temporal propagation approach to track objects detected by a segmentation network. UVO [44] and BURST [2] provide novel datasets and region-proposal-based baselines for the task of open-world video instance segmentation. In this work, we evaluate our approach on the BURST [2] dataset as it is more diverse and allows to separately evaluate common and uncommon classes.

Prompt-based methods. Prompt-based methods rely on prompts, *i.e.*, prior knowledge, to segment objects in videos. Video object segmentation (VOS) [11, 17, 19, 20, 35, 40, 43, 51, 56] is a task where the ground truth segmentations of objects (belonging to any category) in the first frame are available, and act as prompts to track the objects throughout the video. CLIPSeg [31] uses words as prompts, by projecting the words onto the image space following CLIP [38], and calculating a similarity matrix to obtain a segmentation mask for the given word prompt. Prompt-based methods work when one has some prior knowledge on what or where to look for. However, in a true open-world setting, such prior knowledge may not be available. We operate in such a setting.

In this work, we combine the advantages of both prompt-based and prompt-less methods. Notably, we do not require additional prompts from the ground

truth or separate networks. Instead, we use equally spaced points distributed over the video frames and encode them as prompts to discover new objects. Also note, that all the aforementioned methods, prompt-less or prompt-based, assign only a one-word label to the detected object. In contrast, we are interested in generating a rich object-centric caption for the given object in this work.

2.2 Dense Video Object Captioning

Dense video object captioning involves detecting, tracking, and captioning trajectories of objects in a video. For this task, DVOC-DS [58] extends the image-based GRIT [47] and trains it with a mixture of disjoint tasks. In addition, existing video grounding datasets VidSTG [57] and VLN [41] are re-purposed for this task. However, DVOC-DS [58] cannot caption multiple action segments within a single object trajectory because the method produces a single caption for the entire object trajectory. In addition, similar to many other video models [1, 45, 48], DVOC-DS [58] struggles with very long videos and only processes up to 200 frames. The method is further constrained to handle only known object categories and it is unclear how the method extends to an open-world setting.

Unlike DVOC-DS [58], we use open-world object queries to tackle open-world video instance segmentation. Differently, in this work, we also process video-frames sequentially using a short temporal context. Hence, our method is able to process long videos, as well as handle multiple action segments within a single object trajectory. Finally, we leverage masked attention for dense video object captioning, which has not been explored before.

2.3 Contrastive Loss for Object Queries

Many recent approaches have used a contrastive loss to help in video instance segmentation. OWVISFormer [39] uses a contrastive loss in the open-world setting: it ensures that assigned foreground objects are similar to each other while being different from the background objects. IDOL [50] works in the closed-world setting, and uses an interframe contrastive loss to ensure object queries belonging to the same object across frames are similar, and object queries of different instances across frames differ. In contrast, in this work, for both the closed- and open-world setting, we use a contrastive loss to ensure that no two object queries in the foreground are similar to each other, even in the same frame.

2.4 Generalized Video Understanding

Recently, there has been progress in unifying different video related tasks. TubeFormer [23], Unicorn [53], and CAROQ [13] unify different video segmentation tasks in the closed world. DVOC-DS [58] unifies the tasks of detecting closed-world objects in videos and captioning those closed-world objects. In this work, we explore the task of detecting or segmenting both closed- and open-world objects in videos, and captioning these objects.

Video understanding starts from a strong generalized image understanding. Several works generalize multiple image related tasks. Some methods [8, 9, 21] combine different image segmentation methods, and provide a baseline for many

different video understanding tasks [7, 13, 18, 50]. X-Decoder [59] unifies different image segmentation tasks along with the task of referring image segmentation. SAM [24] introduces a vision foundation model, that primarily performs prompt-based open-world image segmentation, and can be used for many downstream tasks. Different from these works, we develop a generalized method for videos that tackles segmentation and object-centric captioning for both open- and closed-world objects.

2.5 Closed-World Video Instance Segmentation

Closed-world video instance segmentation involves simultaneously segmenting and tracking objects from a fixed category-set in a video. Some works [3–5, 12, 16, 32, 36, 42, 52, 54, 55] rely on classical region-based proposals. Recent works [7, 13, 18, 33, 46, 49, 50] rely on query-based proposals and perform significantly better at discovering closed-world objects. Differently, in this work, we explore query-based proposals for both the closed- and open-world setting.

3 Approach

Given a video, our goal is to jointly detect, segment and caption object instances present in the video. Importantly, note that object instance categories may not be part of the training set (*e.g.*, the parachutes shown in Fig. 3 (top row)), placing our goal in an open-world setting. To achieve this goal, a given video is first broken into short clips, each consisting of T frames. Each clip is processed using our approach OW-VISCap. We discuss merging of the results of each clip in Sec. 4.

We provide an overview of OW-VISCap to process each clip in Sec. 3.1. We then discuss our contributions: (a) introduction of open-world object queries in Sec. 3.2, (b) use of masked attention for object-centric captioning in Sec. 3.3, and (c) use of inter-query contrastive loss to ensure that the object queries are different from each other in Sec. 3.4. In Sec. 3.5, we discuss the final training objective.

3.1 Overview

Fig. 2 (left) provides an overview of our approach OW-VISCap. To deal with the open-world setting, *i.e.*, to ensure that we can detect, segment and caption never before seen object instances, we introduce open-world object queries, $q_{ow} \in \mathbb{R}^{N_{obj,ow} \times C}$. These open-world object queries are in addition to closed-world object queries $q_{cw} \in \mathbb{R}^{N_{obj,cw} \times C}$, commonly used in prior work [7, 8, 13, 18, 50]. Here, $N_{obj,ow}$ and $N_{obj,cw}$ are the total number of open-world and closed-world queries, and C refers to the channel dimension for each object query. The open-world object queries are created by encoding a grid of points, which act as prompts, through a prompt encoder (shown in purple in Fig. 2 (left)). Note, that by using open-world object queries, we aim to discover new open-world objects without needing additional prompts from the user, ground-truth or a different network. This allows us to combine the prompt-based and prompt-less methods.

Both open- and closed-world object queries are processed by our specifically designed captioning head which yields an object-centric caption, a classification head which yields a category label, and a detection head which yields either a segmentation mask or a bounding-box.

We compute both sets of object queries (open- and closed-world respectively) from initial embeddings $e_{ow} \in \mathbb{R}^{N_{obj,ow} \times C}$ and $e_{cw} \in \mathbb{R}^{N_{obj,cw} \times C}$. Concretely, to generate meaningful open- and closed-world object queries q_{ow} and q_{cw} , these initial embeddings are continuously modulated in the object transformer (shown in green) by combining them with multi-level image features via masked attention following [7, 8]. The closed-world embeddings e_{cw} are trainable. We discuss the generation of open-world embeddings e_{ow} , the computation of open-world object queries q_{ow} from open-world embeddings e_{ow} and their training in Sec. 3.2.

Fig 2 (right) illustrates our captioning head. It consists of an object-to-text transformer (shown in blue) and a frozen LLM (shown in gray). We use $q_{obj} = [q_{ow}, q_{cw}]$ to denote all the object queries obtained from the object transformer. The i^{th} object query $q_{obj}^i \in \mathbb{R}^{1 \times C}$ is concatenated with learnt text embeddings $e_{text} \in \mathbb{R}^{N_{text} \times C}$, where N_{text} is the total number of text queries. The concatenated object query and text embeddings are continuously modulated in the object-to-text transformer by combining them with image features so as to generate meaningful text queries $q_{text}^i \in \mathbb{R}^{(N_{text}+1) \times C}$ for the i^{th} object. Note, q_{text}^i is used by the frozen LLM to generate object-centric captions. The segmentation mask for the i^{th} object generated in the detection head is used to mask the attention in the object-to-text transformer, as described in Sec. 3.3. We find this design to enable the LLM to generate more object-centric captions.

We introduce an inter-query contrastive loss to ensure that the object queries are encouraged to differ from each other. We provide details in Sec. 3.4. For closed world objects, this loss helps in removing highly overlapping false positives. For open-world objects, it helps in the discovery of new objects.

Finally, we provide the full training objective in Sec. 3.5.

3.2 Open-World Object Queries

To help discover new objects, we introduce open-world object queries q_{ow} in addition to the commonly used closed world object queries. Our open-world object queries are generated from open-world embeddings e_{ow} , which are continuously modulated in the object transformer by combining them with image features via masked attention, following [7, 8]. In the following, we discuss how we compute open-world embeddings e_{ow} via a prompt encoder, and how we design the training loss so as to encourage discovery of new objects.

Prompt encoder. The open-world embeddings e_{ow} are generated in the prompt encoder. An illustration is provided in Fig. 2 (left). We simply encode a grid of equally spaced points along the height and width of the frames of the clip, using the prompt encoder employed in SAM [24]. The use of equally spaced points encourages the open-world object queries to focus on different regions of the video frames, encouraging object discovery throughout the frames. This also encourages the open-world object queries to be diverse from one another.

Open-world loss. To encourage discovery of new objects, we introduce an open-world loss \mathcal{L}_{ow} . It differs in one key-aspect from a classic closed-world loss [7]: we don’t penalize false positive predictions. We elaborate on details and efficacy of this design next.

We first match the ground truth objects with the open-world predictions by minimizing a matching cost using the Hungarian algorithm [34]. The optimal matching is then used to calculate the final open-world loss.

Concretely, consider a set of ground truth objects, padded with a no-object category \emptyset to equal the number of open-world predictions $N_{\text{obj,ow}}$. Let us use $\hat{\sigma}_{\text{ow}}$ to represent the optimal matching between the ground truth objects and the open-world predictions.

The open-world loss is given by

$$\mathcal{L}_{\text{ow}} = \sum_i \mathbb{1}_{c^i \neq \emptyset} [\mathcal{L}_{\text{cls}}(i, \hat{\sigma}_{\text{ow}}^i) + \mathcal{L}_{\text{det}}(i, \hat{\sigma}_{\text{ow}}^i)], \quad (1)$$

where i is the object index. $\mathcal{L}_{\text{cls}}(i, \hat{\sigma}_{\text{ow}}^i)$ is the binary classification loss between the ground truth object with index i and a prediction with index $\hat{\sigma}_{\text{ow}}^i$. This loss helps in classifying a prediction as a foreground object or as background. $\mathcal{L}_{\text{det}}(i, \hat{\sigma}_{\text{ow}}^i)$ is the detection loss (mask loss or bounding box loss) between the ground truth object with index i and a prediction with index $\hat{\sigma}_{\text{ow}}^i$. c^i is the class prediction, which is foreground ($c^i \neq \emptyset$) or background $c^i = \emptyset$ for the open-world setting.

Differently, in the classic closed-world setting, the false positive predictions that are matched with the ground truth no-object category are also penalized. Concretely, there is an additional component $\sum_i \mathbb{1}_{c^i = \emptyset} [\mathcal{L}_{\text{cls}}(i, \hat{\sigma}_{\text{cw}}^i)]$ in the closed-world loss, where $\hat{\sigma}_{\text{cw}}$ refers to the optimal matching between the ground truth objects and the closed-world predictions and $\mathcal{L}_{\text{cls}}(i, \hat{\sigma}_{\text{cw}}^i)$ is the binary classification loss between the ground truth object with index i and a prediction with index $\hat{\sigma}_{\text{cw}}^i$. This differs from the aforementioned open-world setting, where the false positives are important as they act as newly discovered objects.

3.3 Captioning Head

To obtain an object-centric caption, object queries $q_{\text{obj}} = [q_{\text{ow}}, q_{\text{cw}}]$, concatenating the open-world object queries discussed in the previous section and classic closed-world object queries, are processed via our captioning head. Fig 2 (right) illustrates the captioning head. It consists of an object-to-text transformer and a frozen LLM.

To compute a caption, the i^{th} object query q_{obj}^i is concatenated with learnt text embeddings e_{text} . The concatenated result is continuously modulated in the object-to-text transformer by combining it with image features to generate meaningful text queries q_{text}^i for the i^{th} object. Subsequently, q_{text}^i is used by the frozen LLM to generate object-centric captions. The segmentation mask for the i^{th} object generated in the detection head is used to mask the attention in the object-to-text transformer. We find this to enable the LLM to generate more object-centric captions. We provide details next.

Masked attention for object-centric captioning. Masked attention involves attending within the foreground region of the predicted mask for each object query. Concretely, for each object i , we restrict the cross attention in the object-to-text transformer by using the segmentation mask of the object generated by the detection head to generate object-centric text queries q_{text}^i . Intuitively, this enables the model to focus on local object-centric features, which are sufficient to update the text queries. Importantly, note that context information from the video frames can be gathered through the self-attention layers. The proposed design hence doesn't take away any information. It rather provides the same information in clearly separated layers.

Formally, for the i^{th} object we compute the query features $X_l^{\text{cap},i} \in \mathbb{R}^{(N_{\text{text}}+1) \times C}$ obtained from the l^{th} object-to-text transformer layer via

$$X_l^{\text{cap},i} = \text{softmax}(\mathcal{M}^i + Q_l^i K_l^T) V_l + X_{l-1}^{\text{cap},i}. \quad (2)$$

Here, $\mathcal{M}^i \in \{0, -\infty\}^{1 \times HWT}$ is the attention mask in the object-to-text transformer such that at feature location (x, y) , $\mathcal{M}^i(x, y) = 0$, if $M^i(x, y) = 1$ and $\mathcal{M}^i(x, y) = -\infty$, if $M^i(x, y) = 0$. M^i is the binary mask obtained from the detection head. Moreover, $K_l, V_l \in \mathbb{R}^{HWT \times C}$ are the linearly transformed image features. To initialize, we let $X_0^{\text{cap},i} = [q_{\text{obj}}^i, e_{\text{text}}]$, where $q_{\text{obj}}^i \in \mathbb{R}^{1 \times C}$ is the i^{th} object query obtained from the object transformer and $e_{\text{text}} \in \mathbb{R}^{N_{\text{text}} \times C}$ are the learnt text embeddings shown in Fig. 2 and introduced in Sec. 3.1. C is the channel dimension, H, W are the spatial dimensions of the image features and T is the clip-length. N_{text} is the total number of text queries.

We'll show in Sec. 4.3 that the masked attention helps in generating more object-centric captions.

3.4 Inter-Query Contrastive Loss

We introduce an inter-query contrastive loss $\mathcal{L}_{\text{cont}}$ to ensure that the object queries are different from each other, as described next. For closed-world objects, this loss helps in removing highly overlapping false positives. For open-world objects, it helps in the discovery of new objects. Formally,

$$\mathcal{L}_{\text{cont}} = - \sum_{i,j} L(q_{\text{obj}}^i, q_{\text{obj}}^j), \quad (3)$$

where q_{obj}^i and q_{obj}^j are the i^{th} and the j^{th} objects and $i \neq j$. L refers to the L1 distance. Via this loss, we *maximize* the L1 distance between the object queries, *i.e.*, we encourage that the object queries differ from each other.

3.5 Training

Our total training loss is

$$\mathcal{L}_{\text{total}} = \mathcal{L}_{\text{ow}} + \mathcal{L}_{\text{cont}} + \mathcal{L}_{\text{cap}} + \mathcal{L}_{\text{cw}}.$$

Here, \mathcal{L}_{ow} is the open-world loss as discussed in Sec. 3.2 and $\mathcal{L}_{\text{cont}}$ is the inter-query contrastive loss discussed in Sec. 3.4. \mathcal{L}_{cap} is the standard captioning

Table 1: Open-world tracking accuracy (OWTA) on the BURST validation and test sets for all, common (comm.) and uncommon (unc.) categories of objects. Onl. refers to online frame-by-frame processing. The best scores are highlighted in bold font, and the second-best scores are underlined.

Method	Validation (OWTA)			Test (OWTA)		
	all	comm.	unc.	all	comm.	unc.
OWTB [28]	55.8	59.8	38.8	56.0	59.9	38.3
Mask2Former [8]+STCN [11]	64.6	71.0	25.0	57.5	62.9	23.9
Mask2Former [8]+DEVA [10] (onl.)	69.5	74.6	42.3	70.1	75.0	44.1
EntitySeg [37]+DEVA [10] (onl.)	68.8	72.7	<u>49.6</u>	<u>69.5</u>	<u>72.9</u>	<u>53.0</u>
OW-VISCap (ours) + DEVA [10] (onl.)	<u>69.0</u>	<u>73.5</u>	55.2	69.2	72.4	57.2

Table 2: Dense video object captioning results on the VidSTG [57] dataset. Off. indicates offline methods and onl. refers to online methods.

Method	Mode	CHOTA	DetA	AssA	CapA	AP _M
DVOC-DS (joint training) [58]	off.	51.6	65.5	56.9	36.8	69.3
DVOC-DS (disjoint training) [58]	off.	28.0	45.9	48.0	10.0	39.8
OW-VISCap (ours)	onl.	53.0	60.1	54.0	43.9	62.6

loss introduced by DVOC-DS [58]. \mathcal{L}_{cw} is the closed-world loss following prior work [8]. In order to compute \mathcal{L}_{cw} , the ground truth objects are first matched with the closed-world objects; the optimal matching is used to compute the final closed-world loss \mathcal{L}_{cw} . This closed-world loss involves penalizing the false positive predictions, which is different from \mathcal{L}_{ow} . Note that in our setting, the ground truth objects are matched twice, once with the open-world object queries to compute \mathcal{L}_{ow} , and once with the closed-world object queries to compute \mathcal{L}_{cw} .

4 Experiments

We evaluate our proposed approach on the diverse tasks of open-world video instance segmentation (OW-VIS), dense video object captioning (Dense VOC), and closed-world video instance segmentation (VIS). Note that there is no dedicated dataset for the task of open-world video instance segmentation and captioning. Hence we use the three aforementioned tasks and evaluate the three different aspects of our approach: open-world capability, video object captioning, and video instance segmentation. In the following subsections, we first discuss the datasets and evaluation metrics used in our evaluation in Sec. 4.1. We then compare our performances to baselines in Sec. 4.2. We demonstrate how each of our contributions results in better performance through an ablation study in Sec. 4.3. Finally we show some qualitative results in Sec. 4.4.

4.1 Datasets and Evaluation Metrics

We evaluate our approach on the OW-VIS, Dense VOC and VIS tasks. For OW-VIS, we use the challenging BURST dataset [2]. For the Dense VOC task,

Table 3: Results on the OVIS [36] validation data. All methods use the ResNet-50 backbone. The best performing methods are highlighted in bold font. The second best methods are underlined.

Method	AP	AP ₅₀	AP ₇₅	AR ₁	AR ₁₀
MaskTrack [54]	10.8	25.3	8.5	7.9	14.9
DeVIS [6]	23.7	47.6	20.8	12.0	28.9
MinVIS [18]	25.0	45.5	<u>24.0</u>	13.9	29.7
VMT [22]	16.9	36.4	13.7	10.4	22.7
InstanceFormer [25]	20.0	40.7	18.1	12.0	27.1
VITA [15]	19.6	41.2	17.4	11.7	26.0
CAROQ [13]	25.8	47.9	25.4	<u>14.2</u>	33.9
OW-VISCap (w/o $\mathcal{L}_{\text{cont}}$)	23.2	45.2	21.7	13.5	30.1
OW-VISCap (ours)	<u>25.4</u>	48.8	22.8	14.3	<u>32.8</u>

Table 4: Ablation on the BURST [2] validation data. ‘w/o q_{ow} ’ refers to without open-world object queries; ‘w/o $\mathcal{L}_{\text{cont}}$ ’ refers to without contrastive loss.

Method	OWTA		
	all	comm.	unc.
Ours	55.5	58.2	43.8
w/o q_{ow}	54.3	57.9	41.2
w/o $\mathcal{L}_{\text{cont}}$	53.5	56.1	41.6

Table 5: Ablation on the VidSTG [57] data. ‘w/o m.a.’ refers to without masked attention. ‘bb. cap.’ and ‘en. bb. cap.’ refers to bounding box captioning and enlarged bounding box captioning.

Method	CHOTA	DetA	AssA	CapA
Ours	51.0	56.1	54.0	43.9
w/o m.a.	39.5	56.1	54.0	20.3
bb. cap.	48.9	56.1	54.0	38.6
en. bb. cap.	49.4	56.1	54.0	40.4

we use the VidSTG dataset [57]. Note that VidSTG [57] has bounding box and tracking identity for all objects, but captions are not exhaustively provided. However, DVOC-DS [58] uses VidSTG [57] for the Dense VOC task by removing the captioning loss for missing captions during training and not evaluating the missing captions during evaluation. We follow a similar setting. For the VIS task, we evaluate on the OVIS dataset [36].

For OW-VIS, we use the standard evaluation metrics of open-world tracking accuracy (OWTA) [2] for all, common and uncommon categories. For Dense VOC, we use the captioned higher order tracking accuracy (CHOTA) [58], which depends on the detection accuracy (DetA), association accuracy (AssA), and captioning accuracy (CapA). We also report the frame-based METEOR score (AP_M). For VIS, we use the standard evaluation metrics of average precision (AP, AP₅₀, AP₇₅) and average recall (AR₁, AR₁₀) [54].

4.2 Main Results

Open-world video instance segmentation (BURST). Tab. 1 shows our results for the OW-VIS task on the BURST dataset [2]. We report the open-world tracking accuracy for all, common (comm.) and uncommon (unc.) categories. For the uncommon classes, we achieve the state-of-the-art, improving upon the next best method (Mask2Former [8]+DEVA [10]) by ~ 6 points on

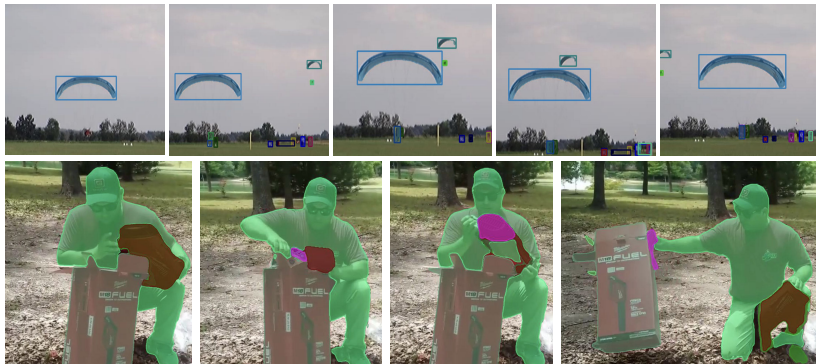


Fig. 3: Example from the BURST validation data. The masks are superimposed on the objects. The top-row shows examples of parachutes in the air and people on the grass. The parachutes belong to the uncommon object category, *i.e.*, parachutes were never seen during training. Our approach is able to detect and retain the identity of the blue and the green parachutes as the green crosses the blue parachute. The bottom row shows a person unboxing a leaf blower. The carton of the leaf blower (gray mask), the leaf blower (maroon mask) and the plastic wrapper (pink mask) are never seen during training. We are able to consistently detect and track them along with the person (common object category during training).

the BURST [2] validation data and by ~ 4 points on the BURST test data. For the common categories, our method ranks 2nd in the BURST validation data. We use a SwinL [29] backbone, a clip-length of $T = 1$, and DEVA [10] for the temporal association of objects.

Dense video object captioning (VidSTG). Tab. 2 shows our results on the Dense VOC task. We outperform DVOS-DS [58] on the captioning accuracy (CapA), demonstrating that our captioning head with masked attention (Sec. 3.3) is effective in generating object-centric captions. We improve upon DS-VOC on the overall CHOTA metric, even though we slightly underperform on DetA and AssA. Note that DVOS-DS is an offline method: the entire object trajectories are used for generating the captions. Hence DVOS-DS cannot process videos with more than 200 frames. This is in contrast to our online method, where we sequentially process short video clips of length $T = 2$. This enables to process very long videos. DVOS-DS uses a ViT [14] backbone, whereas we use SwinL [29], which leads to a difference in DetA scores. We use a clip-length $T = 2$ for this experiment. Note that $T = 2$ enables the object queries to be spatio-temporally rich. This helps in generating better object-centric captions. For tracking, we use CAROQ [13] to propagate object queries across frames.

Video instance segmentation (OVIS). Tab. 3 shows our results for the closed-world video instance segmentation task on the OVIS [36] dataset. In the closed-world setting, we disable the open-world object queries. We notice that the contrastive loss $\mathcal{L}_{\text{cont}}$ (discussed in Sec. 3.4) improves the closed-world results. We use a clip-length of $T = 2$ in this setting and CAROQ [13] to combine results from video clips.

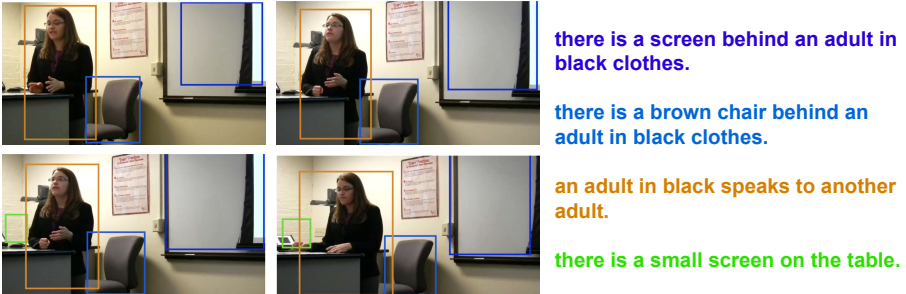


Fig. 4: An example from the VidSTG data. Our approach is able to detect and track objects in the scene consistently and to generate meaningful object-centric captions for each of the detected objects.

4.3 Ablation Studies

Open-world object queries. Tab. 4 (first and second rows) shows how the open-world object queries q_{ow} , described in Sec. 3.2, help in discovering new objects. In Tab. 4, ‘w/o q_{ow} ’ refers to the setting without open-world object queries, *i.e.*, we only use the closed-world object queries to find the common (comm.) and uncommon (unc.) objects. We observe that the performance drops by 2.6 for uncommon categories and by 0.3 points for common categories in ‘w/o q_{ow} ’ as compared to ‘Ours’, where both the open- and closed-world object queries are used.

Masked attention. Tab. 5 shows that masked attention in the object-to-text transformer of the captioning head, described in Sec. 3.3, helps in object-centric captioning using the VidSTG [57] data.

The second row ‘w/o m.a.’ of Tab. 5 refers to the setting without masked attention, *i.e.*, the entire image-feature is used to calculate the cross-attention in the object-to-text-transformer. The object-centric context is only accumulated by concatenating the i^{th} object query with the learnt text embeddings, as discussed in Sec. 3.3 and shown in Fig. 2. We observe that the captioning accuracy CapA drops by 23 points, indicating that concatenating the object query with the text embeddings is not sufficient for an object-centric focus.

The third row in Tab. 5, ‘bb. cap.’ (bounding box captioning), pursues the opposite setting. Here, the images are cropped based on the object bounding box predictions in the detection head. The cropped images are directly used for captioning, ensuring that both the self and cross attention blocks in the object-to-text transformer operate on object-centric features. Note, that we don’t use masked attention in this setting. We see a drop in CapA of 5 points in this setting. Although the cropping helps in retaining the object-centric information, the overall context from the entire image is missing.

The fourth row in Tab. 5, ‘en. bb. cap.’ (enlarged bounding box captioning), shows a similar setting as the third row, but the bounding boxes are first enlarged by 10% to provide more overall image context. The enlarged bounding boxes are then used to crop the images for captioning. We observe a drop in CapA of 3

points in this setting, indicating that enlarging the bounding boxes helps but is not sufficient to provide overall context.

The first row in Tab. 5, ‘Ours’ (our approach), where we retain the overall context using self attention in the object-to-text transformer and focus on the object-centric features using masked cross attention, performs the best among these settings.

Contrastive loss. Tab. 4 (first and last rows) shows how the contrastive loss $\mathcal{L}_{\text{cont}}$, described in Sec. 3.4, helps in detecting both the common (comm.) and uncommon (unc.) categories of objects. The performance drops by ~ 2 points for both the common and uncommon categories for the setting ‘w/o $\mathcal{L}_{\text{cont}}$ ’, *i.e.*, when the contrastive loss is not used. The contrastive loss helps in removing highly overlapping false positives in the closed-world setting and in discovering new objects in the open-world setting. Tab. 3 further shows that the contrastive loss helps in detecting objects in the closed-world setting.

4.4 Qualitative Results

We provide qualitative results generated by OW-VISCap in this section. Fig. 1 shows an example from the BURST [2] dataset. OW-VISCap is able to simultaneously detect, track and caption objects in the given video frames. The objects belong to both the open- and closed-world. Note that the BURST [2] dataset doesn’t have object-centric captions available for training or evaluation, hence our captioning head was not trained on BURST [2]. We train the captioning head on the Dense VOC task (whose results are shown in Tab. 2). We find this captioning-head to be effective in generating meaningful object-centric captions even for objects never seen during training. Fig. 3 shows two examples from the BURST validation data. We are able to consistently detect, segment, and track the previously seen and unseen objects. Fig. 4 shows an example from the VidSTG [57] data. Our approach is able to detect and track objects in the scene consistently, and to generate meaningful object-centric captions for each of the detected objects.

5 Conclusion

In this work, we introduce OW-VISCap to *jointly detect, segment, track, and caption previously seen or unseen objects in videos*. We introduce open-world object queries to encourage discovery of previously unseen objects without the need of additional user-inputs. Instead of assigning a fixed label to detected objects, we generate rich object-centric captions for each object by using masked attention in an object-to-text transformer. Further, we introduce an inter-query contrastive loss to ensure that the object queries differ from one another. Our approach mostly matches or surpasses the state-of-the-art on the diverse tasks of open-world video instance segmentation on the BURST dataset, dense video object captioning on the VidSTG dataset, and closed-world video instance segmentation on the OVIS dataset. Through an ablation study, we demonstrate the effectiveness of each of our proposed components.

Acknowledgements: This work is supported in part by Agriculture and Food Research Initiative (AFRI) grant no. 2020-67021-32799/project accession no. 1024178 from the USDA National Institute of Food and Agriculture: NSF/USDA National AI Institute: AIFARMS. We also thank the Illinois Center for Digital Agriculture for seed funding for this project. Work is also supported in part by NSF under Grants 2008387, 2045586, 2106825, MRI 1725729.

References

1. Arnab, A., Deghani, M., Heigold, G., Sun, C., Lučić, M., Schmid, C.: Vivit: A video vision transformer. In: ICCV (2021)
2. Athar, A., Luiten, J., Voigtlaender, P., Khurana, T., Dave, A., Leibe, B., Ramanan, D.: Burst: A benchmark for unifying object recognition, segmentation and tracking in video. In: WACV (2023)
3. Athar, A., Mahadevan, S., Osep, A., Leal-Taixé, L., Leibe, B.: Stem-seg: Spatio-temporal embeddings for instance segmentation in videos. In: ECCV (2020)
4. Bertasius, G., Torresani, L.: Classifying, segmenting, and tracking object instances in video with mask propagation. In: ICCV (2020)
5. Braso, G., Leal-Taixé, L.: Learning a neural solver for multiple object tracking. In: CVPR (June 2020)
6. Caelles, A., Meinhardt, T., Brasó, G., Leal-Taixé, L.: Devis: Making deformable transformers work for video instance segmentation. arXiv preprint arXiv:2207.11103 (2022)
7. Cheng, B., Choudhuri, A., Misra, I., Kirillov, A., Girdhar, R., Schwing, A.G.: Mask2former for video instance segmentation. arXiv preprint arXiv:2112.10764 (2021)
8. Cheng, B., Misra, I., Schwing, A.G., Kirillov, A., Girdhar, R.: Masked-attention mask transformer for universal image segmentation. In: CVPR (2022)
9. Cheng, B., Schwing, A.G., Kirillov, A.: Per-pixel classification is not all you need for semantic segmentation. In: NeurIPS (2021)
10. Cheng, H.K., Oh, S.W., Price, B., Schwing, A., Lee, J.Y.: Tracking anything with decoupled video segmentation. In: ICCV (2023)
11. Cheng, H.K., Tai, Y.W., Tang, C.K.: Rethinking space-time networks with improved memory coverage for efficient video object segmentation. In: NeurIPS (2021)
12. Choudhuri, A., Chowdhary, G., Schwing, A.G.: Assignment-space-based multi-object tracking and segmentation. In: ICCV (2021)
13. Choudhuri, A., Chowdhary, G., Schwing, A.G.: Context-aware relative object queries to unify video instance and panoptic segmentation. In: CVPR (2023)
14. Dosovitskiy, A., Beyer, L., Kolesnikov, A., Weissenborn, D., Zhai, X., Unterthiner, T., Deghani, M., Minderer, M., Heigold, G., Gelly, S., et al.: An image is worth 16x16 words: Transformers for image recognition at scale. arXiv preprint arXiv:2010.11929 (2020)
15. Heo, M., Hwang, S., Oh, S.W., Lee, J.Y., Kim, S.J.: Vita: Video instance segmentation via object token association. arXiv preprint arXiv:2206.04403 (2022)
16. Hornakova, A., Henschel, R., Rosenhahn, B., Swoboda, P.: Lifted disjoint paths with application in multiple object tracking. In: ICML (2020)
17. Hu, Y.T., Huang, J.B., Schwing, A.G.: Videomatch: Matching based video object segmentation. In: ECCV (2018)

18. Huang, D.A., Yu, Z., Anandkumar, A.: Minvis: A minimal video instance segmentation framework without video-based training. In: *NeurIPS* (2022)
19. Huang, X., Xu, J., Tai, Y.W., Tang, C.K.: Fast video object segmentation with temporal aggregation network and dynamic template matching. In: *CVPR* (2020)
20. Huang, X., Xu, J., Tai, Y.W., Tang, C.K.: Fast video object segmentation with temporal aggregation network and dynamic template matching. In: *CVPR* (2020)
21. Jain, J., Li, J., Chiu, M.T., Hassani, A., Orlov, N., Shi, H.: Oneformer: One transformer to rule universal image segmentation. In: *CVPR* (2023)
22. Ke, L., Ding, H., Danelljan, M., Tai, Y.W., Tang, C.K., Yu, F.: Video mask transfiner for high-quality video instance segmentation. In: *ECCV* (2022)
23. Kim, D., Xie, J., Wang, H., Qiao, S., Yu, Q., Kim, H.S., Adam, H., Kweon, I.S., Chen, L.C.: Tubeformer-deeplab: Video mask transformer. In: *ICCV* (2022)
24. Kirillov, A., Mintun, E., Ravi, N., Mao, H., Rolland, C., Gustafson, L., Xiao, T., Whitehead, S., Berg, A.C., Lo, W.Y., et al.: Segment anything. *arXiv preprint arXiv:2304.02643* (2023)
25. Koner, R., Hannan, T., Shit, S., Sharifzadeh, S., Schubert, M., Seidl, T., Tresp, V.: Instanceformer: An online video instance segmentation framework. *arXiv preprint arXiv:2208.10547* (2022)
26. Li, J., Li, D., Savarese, S., Hoi, S.: Blip-2: Bootstrapping language-image pre-training with frozen image encoders and large language models. *arXiv preprint arXiv:2301.12597* (2023)
27. Liu, Y., Zulfikar, I.E., Luiten, J., Dave, A., Ramanan, D., Leibe, B., Ošep, A., Leal-Taixé, L.: Opening up open world tracking. In: *CVPR* (2022)
28. Liu, Y., Zulfikar, I.E., Luiten, J., Dave, A., Ramanan, D., Leibe, B., Ošep, A., Leal-Taixé, L.: Opening up open world tracking. In: *Proceedings of the IEEE/CVF Conference on Computer Vision and Pattern Recognition*. pp. 19045–19055 (2022)
29. Liu, Z., Lin, Y., Cao, Y., Hu, H., Wei, Y., Zhang, Z., Lin, S., Guo, B.: Swin transformer: Hierarchical vision transformer using shifted windows. In: *ICCV* (2021)
30. Loshchilov, I., Hutter, F.: Decoupled weight decay regularization. *arXiv preprint arXiv:1711.05101* (2017)
31. Lüddecke, T., Ecker, A.: Image segmentation using text and image prompts. In: *CVPR* (2022)
32. Luiten, J., Fischer, T., Leibe, B.: Track to reconstruct and reconstruct to track. *RAL* (2020)
33. Meinhardt, T., Kirillov, A., Leal-Taixe, L., Feichtenhofer, C.: Trackformer: Multi-object tracking with transformers. In: *CVPR* (2022)
34. Munkres, J.: Algorithms for the assignment and transportation problems. *J-SIAM* (1957)
35. Oh, S.W., Lee, J.Y., Xu, N., Kim, S.J.: Video object segmentation using space-time memory networks. In: *ICCV* (2019)
36. Qi, J., Gao, Y., Hu, Y., Wang, X., Liu, X., Bai, X., Belongie, S., Yuille, A., Torr, P.H., Bai, S.: Occluded video instance segmentation. *arXiv preprint arXiv:2102.01558* (2021)
37. Qi, L., Kuen, J., Wang, Y., Gu, J., Zhao, H., Torr, P., Lin, Z., Jia, J.: Open world entity segmentation. *PAMI* (2022)
38. Radford, A., Kim, J.W., Hallacy, C., Ramesh, A., Goh, G., Agarwal, S., Sastry, G., Askell, A., Mishkin, P., Clark, J., et al.: Learning transferable visual models from natural language supervision. In: *ICML* (2021)
39. Thawakar, O., Narayan, S., Cholakkal, H., Anwer, R.M., Khan, S., Laaksonen, J., Shah, M., Khan, F.S.: Video instance segmentation in an open-world. *arXiv preprint arXiv:2304.01200* (2023)

40. Voigtlaender, P., Chai, Y., Schroff, F., Adam, H., Leibe, B., Chen, L.C.: Feelvos: Fast end-to-end embedding learning for video object segmentation. In: CVPR (2019)
41. Voigtlaender, P., Changpinyo, S., Pont-Tuset, J., Soricut, R., Ferrari, V.: Connecting vision and language with video localized narratives. In: CVPR (2023)
42. Voigtlaender, P., Krause, M., Ošep, A., Luiten, J., Sekar, B.B.G., Geiger, A., Leibe, B.: MOTs: Multi-object tracking and segmentation. In: CVPR (2019)
43. Wang, Q., Zhang, L., Bertinetto, L., Hu, W., Torr, P.H.: Fast online object tracking and segmentation: A unifying approach. In: CVPR (2019)
44. Wang, W., Feiszli, M., Wang, H., Tran, D.: Unidentified video objects: A benchmark for dense, open-world segmentation. In: ICCV (2021)
45. Wang, Y., Xu, Z., Wang, X., Shen, C., Cheng, B., Shen, H., Xia, H.: End-to-end video instance segmentation with transformers. In: CVPR (2021)
46. Wang, Y., Xu, Z., Wang, X., Shen, C., Cheng, B., Shen, H., Xia, H.: End-to-end video instance segmentation with transformers. In: CVPR (2021)
47. Wu, J., Wang, J., Yang, Z., Gan, Z., Liu, Z., Yuan, J., Wang, L.: Grit: A generative region-to-text transformer for object understanding. arXiv preprint arXiv:2212.00280 (2022)
48. Wu, J., Jiang, Y., Sun, P., Yuan, Z., Luo, P.: Language as queries for referring video object segmentation. In: CVPR (2022)
49. Wu, J., Jiang, Y., Zhang, W., Bai, X., Bai, S.: Seqformer: a frustratingly simple model for video instance segmentation. arXiv preprint arXiv:2112.08275 (2021)
50. Wu, J., Liu, Q., Jiang, Y., Bai, S., Yuille, A., Bai, X.: In defense of online models for video instance segmentation. In: ECCV (2022)
51. Xu, N., Yang, L., Fan, Y., Yang, J., Yue, D., Liang, Y., Price, B., Cohen, S., Huang, T.: Youtube-vos: Sequence-to-sequence video object segmentation. In: ECCV (2018)
52. Xu, Z., Zhang, W., Tan, X., Yang, W., Huang, H., Wen, S., Ding, E., Huang, L.: Segment as points for efficient online multi-object tracking and segmentation. In: ECCV (2020)
53. Yan, B., Jiang, Y., Sun, P., Wang, D., Yuan, Z., Luo, P., Lu, H.: Towards grand unification of object tracking. In: ECCV (2022)
54. Yang, L., Fan, Y., Xu, N.: Video instance segmentation. In: ICCV (2019)
55. Yang, S., Fang, Y., Wang, X., Li, Y., Fang, C., Shan, Y., Feng, B., Liu, W.: Crossover learning for fast online video instance segmentation. In: ICCV (2021)
56. Zhang, L., Lin, Z., Zhang, J., Lu, H., He, Y.: Fast video object segmentation via dynamic targeting network. In: ICCV (2019)
57. Zhang, Z., Zhao, Z., Zhao, Y., Wang, Q., Liu, H., Gao, L.: Where does it exist: Spatio-temporal video grounding for multi-form sentences. In: CVPR (2020)
58. Zhou, X., Arnab, A., Sun, C., Schmid, C.: Dense video object captioning from disjoint supervision. arXiv preprint arXiv:2306.11729 (2023)
59. Zou, X., Dou, Z.Y., Yang, J., Gan, Z., Li, L., Li, C., Dai, X., Behl, H., Wang, J., Yuan, L., et al.: Generalized decoding for pixel, image, and language. In: CVPR (2023)

Supplementary Material — OW-VISCap: Open-World Video Instance Segmentation and Captioning



Fig. S1: Results on the BURST dataset. We successfully segment and track closed-world objects (e.g., persons), and open-world objects (e.g., rackets), throughout the video.

This is the supplementary material of the OW-VISCap paper. We develop OW-VISCap, an approach for open-world video instance segmentation and captioning. We test our approach on the task of open-world video instance segmentation (OW-VIS), dense video object captioning (Dense VOC) and closed-world video instance segmentation (VIS) in Sec. 4.

In this supplementary material, we provide additional analysis (Sec. A) to support the contributions we made in Sec. 3 of the main paper. We then discuss the implementation details (Sec. B) and limitations (Sec. C) of our approach.

Fig. S1 shows additional results on the BURST [2] dataset. We successfully segment and track the closed-world objects: persons, and the open-world objects: rackets, throughout the video. Fig. S2 shows results on the VidSTG [57] dataset. The detected objects are tracked throughout the video and our method generates meaningful captions for each object.

A Additional Analysis

In this section we provide additional analysis on the different components discussed in Sec. 3 of the main paper.

A.1 Open-World Embeddings as Object Proposals

We introduced open-world embeddings e_{ow} in Sec. 3.2 of the main paper. These embeddings are modulated in the object transformer (Fig. 2) to generate open-world object queries. We obtain the open-world embeddings by encoding a grid of



a child in blue speaks to an adult in the room.
an adult in black hugs a baby in the room.

Fig. S2: Results on the VidSTG dataset. Our approach detects, tracks and generates meaningful object-centric captions for each object throughout the video.

equally spaced points across the feature dimensions through a prompt encoder. This encourages object discovery throughout the video-frame. The open-world embeddings act as initial abstract object proposals.

In Fig. S3, we show that the open-world embeddings are strong object proposals, even before they are modulated by the object transformer by being combined with video frame features. The person, the spoon, the plate, and some food on the plate are discovered by the open-world embeddings. Their segmentation masks are obtained by the dot product between the open-world embeddings and the video frame features. Further, we see a strong spatial correlation between the grid of points and the segmentation masks generated by the corresponding open-world embeddings. This suggests that encoding a grid of points throughout the feature dimensions encourages object discovery throughout the video frames.

A.2 Masked Attention for Object-Centric Captioning

In Tab. 5, we quantitatively show that masked-attention (Sec. 3.3) helps in generating accurate object-centric captions for individual objects. Fig. S4 shows the high quality of the object-centric captions generated. The black caption (‘a family sitting on a couch with a child’) is obtained when no mask is provided in the object-to-text transformer. The entire image features are seen during the cross attention operation in each layer of the object-to-text transformer. The caption fails to capture the object-centric details.

The colored captions are generated with masked-attention for the individual objects. The colored captions on the left clearly highlight the effectiveness of masked attention to generate object-centric captions. For example, the three persons (highlighted in cyan, grayish blue, and green) have distinct captions, each one describing the individual identities of the corresponding person. The school bag (light blue) is also described correctly. We want to note that sometimes the method fails to generate meaningful object-centric captions for small objects (captions on the right). We discuss this more in Sec. C.

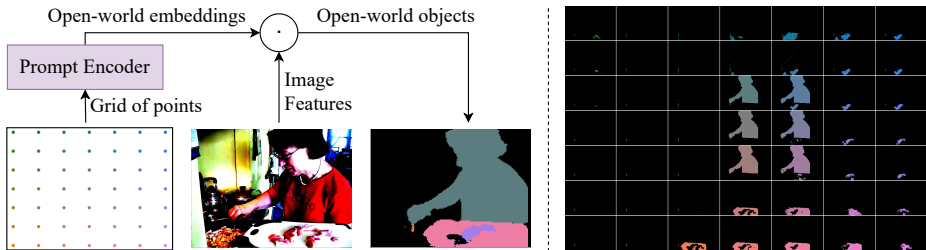


Fig. S3: Open-world embeddings act as strong object proposals. Further, a strong spatial correlation exists between the grid of points and the segmentation masks generated by the corresponding open-world embeddings. This is highlighted by the color of the points in the grid, and the color of the segmentation masks.



a family sitting on a couch with a child.

back of the school bag.

the mother is sitting on the couch.

a child is sitting on a couch.

a man is sitting on a couch with wife and child.

a family sits on the couch.

the the the the the the the

Fig. S4: Masked attention helps generate object-centric captions (colored captions on the left). Providing no mask during cross attention fails to capture object centric details (black caption). However, masked-attention sometimes fails to generate meaningful object-centric captions for small objects (colored captions on the right).

A.3 Contrastive Loss to Suppress Overlapping Predictions

In Tab. 3 and Tab. 4 of the main paper, we demonstrate the effectiveness of using the contrastive loss $\mathcal{L}_{\text{cont}}$ (discussed in Sec. 3.4) for object detection. This loss encourages that object queries differ from each other, among others by suppressing highly overlapping predictions. We highlight this in Fig. S5. The left image shows a frame from the OVIS [36] dataset. The top-right and bottom-right images show a few predictions from our network trained without (top) and trained with (bottom) the contrastive loss. The repetitive predictions for the top-right image are highlighted with red and cyan boxes. The contrastive loss helps in removing these repetitions.

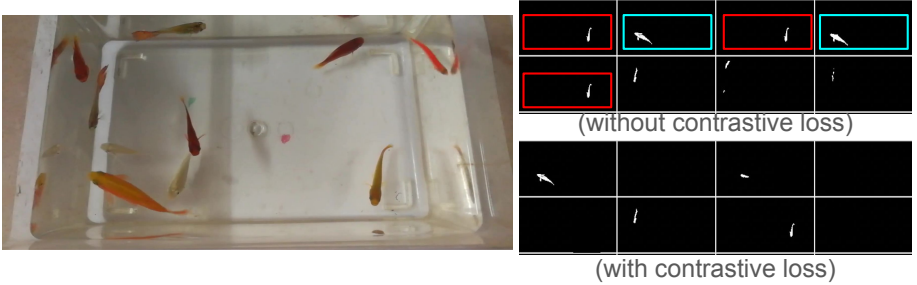


Fig. S5: The repetitive predictions without contrastive loss (top-right) are highlighted with red and cyan boxes. Contrastive loss (bottom-right) helps in suppressing these repetitions.

B Implementation Details

In this section, we provide the implementation details of OW-VISCap. We first describe the architecture of different components discussed in Sec. 3. We then discuss our choice of hyper-parameters for all experiments discussed in Sec. 4. We also discuss the resources and the licenses of the code-bases and datasets used in the paper.

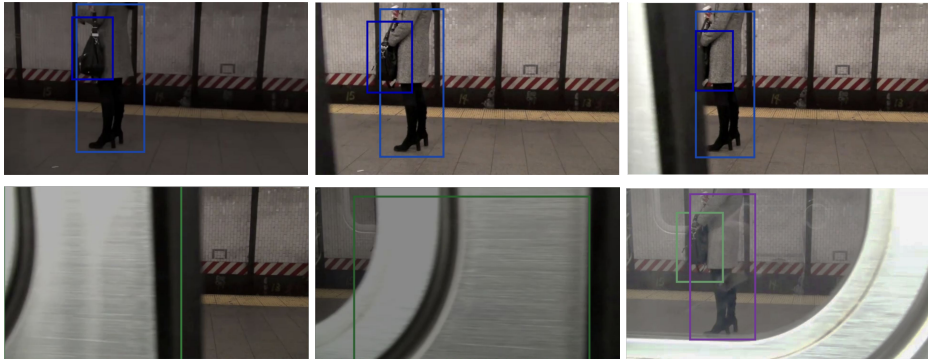
B.1 Architecture

Prompt encoder. Our prompt encoder discussed in Sec. 3.2 is a lightweight network, following the architecture of the prompt encoder used in SAM [24]. We initialize our prompt encoder from SAM [24] and fine-tune it on the BURST [2] dataset.

Captioning head. Our captioning head discussed in Sec. 3.3 consists of an object-to-text transformer and a frozen large language model (LLM). The object-to-text transformer decoder has 11 transformer layers. Each layer has a self attention, masked cross attention (discussed in Sec. 3.3) operations, followed by a feed forward network. The object-to-text transformer and the text embeddings e_{text} are initialized from BLIP-2 [26]. We use a frozen OPT-2.7B model as the LLM. We fine-tune the object-to-text transformer and the text embeddings on the VidSTG [57] dataset.

B.2 Hyper-Parameters

We now discuss the hyper-parameters used in this work. For experiments on the BURST [2] dataset, we encode a grid of 7×7 point across the width and height of the image features to obtain the open-world embeddings e_{ow} discussed in Sec. 3.2. Hence the total number of open-world object queries $N_{\text{obj,ow}}$ is 49. We also experimented with a grid of 4×4 and 10×10 , but didn't see a significant change in performance. For experiments on the VidSTG [57] dataset, the number



an adult in gray clothes carries a black bag
 there is a black handbag behind an adult woman.
 there is a silver train behind an adult in black clothes
 an adult in gray clothes
 an adult is holding a black dog

Fig. S6: A failure mode, where the object identities aren’t retained after prolonged occlusion. After a train crosses the screen for a prolonged period of time (~ 30 frames), the person initially identified as blue is identified as green, and the bag is later identified as light green instead of dark blue. The last caption for the bag is also erroneous.

of text embeddings e_{text} is 32. In all experiments, the maximum number of closed world objects ($N_{\text{obj,cw}}$) in a given video for a ResNet-50 backbone is 100, and for a Swin-L backbone is 200. We use a feature dimension C (Sec. 3.1) of 256 in all models.

We trained the models with an initial learning rate of 0.0001 and ADAMW [30] optimizer with a weight decay of 0.05. We use a batch size of 8. The networks were first initialized with weights from Mask2Former [8] trained on the COCO image instance segmentation dataset. We then fine-tune the models on the respective BURST [2], VidSTG [57], and OVIS [36] datasets for 10,000, 16,000 and 8,000 iterations respectively.

B.3 Resources

We used 8 NVIDIA A100 GPUs to run the experiments presented in this paper. Each experiment took roughly 10 GPU hours of training on the A100 GPUs for the BURST experiments, 16 GPU hours for the VidSTG experiments, and 8 GPU hours for the VIS dataset experiments.

B.4 Licenses

Our code is built on Mask2Former [8] which is majorly licensed under the MIT license, with some portions under the Apache-2.0 License. We also build on SAM [24], which is released under the Apache 2.0 License and BLIP-2 [26]

which is released under the MIT license. The OVIS [36] dataset is released under the Attribution-NonCommercial-ShareAlike (CC BY-NC-SA) License. The VidSTG [57] and BURST [2] datasets are released under the MIT license.

C Limitations

In this section, we show some failure modes of our proposed approach and discuss limitations. Fig. S3 shows that our approach sometimes fails to detect some open-world objects that a human may find to be of interest. For example, the grinder on the left, the window at the top-right, *etc.*, are not detected by the network. The colored captions on the right side of Fig. S4 show that our approach sometimes fails to generate meaningful object-centric captions for small objects. For the purple object (cushion on a sofa), the caption (‘the the the ...’) is not meaningful since it fails to form a complete sentence or capture the identity of the object it represents. For the red object (other cushions on a sofa), the caption (‘a family sits on the couch’) is not object-centric since it fails to provide a description specific to the object. Fig. S6 further highlights a failure mode. After a train crosses the scene for a prolonged period of time (~ 30 frames), object identities may be lost.

These issues can be addressed by stronger strategies for open-world object discovery, stronger caption-generators, and integrating better object trackers, which we leave for future work.